Effect of Zn nanoparticle-doped flux on mechanical properties of SAC305 solder joint after electromigration

M. Nasir Bashir[1,*], Niaz Bahadur Khan[1], Shahid Bashir[2], Abdul Faheem Khan[3], M. M. Quazi[4], Mustabshirha Gul[5], Saif Wakeel[6], and Hafiz Muhammad Saad[1]

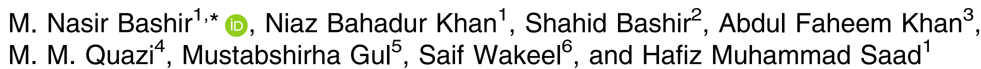

[1] *National University of Sciences and Technology, Islamabad, Pakistan*
[2] *Higher Institution Centre of Excellence (HICoE), UM Power Energy Dedicated Advanced Centre (UMPEDAC), Level 4, Wisma R&D, Universiti Malaya, Jalan Pantai Baharu, 59990 Kuala Lumpur, Malaysia*
[3] *Department of Materials Science and Engineering, Institute of Space Technology, 1-National Highway, Islamabad 44000, Pakistan*
[4] *Faculty of Mechanical and Automotive Engineering Technology, Universiti Malaysia Pahang, 26600 Pekan, Pahang, Malaysia*
[5] *Mechanical Engineering department, Faculty of Engineering and Technology, Bahauddin Zakariya University, Multan 60000, Pakistan*
[6] *Tyndall National Institute, University College Cork, Cork T12R5CP, Ireland*

Received: 7 October 2022
Accepted: 13 December 2022
Published online: 31 January 2023

© The Author(s), under exclusive licence to Springer Science+Business Media, LLC, part of Springer Nature 2023

ABSTRACT

Migration of Cu atoms from the cathode side to the anode side causes void formation in the solder joint, which is the root cause of electromigration failures in lead-free solder joints. This study investigates the effects of Zn nanoparticle-doped flux on the mechanical properties of SAC305 solder joint under high current density. Nanoparticle-doped flux is a novel technique which mainly focused to modify the interfaces of the solder joint. Since, electromigration mainly damages the interfaces of the solder joint, so nanoparticle-doped flux technique was used to retard the electromigration damages. Electromigration test was conducted under the current density of 1×10^4 A/cm^2. The electromigration test was conducted in the silicon oil bath at a maintained temperature of 80 ± 5 °C. Tensile test was conducted before and after electromigration tests for undoped and Zn nanoparticle-doped solder joints. The results showed that the mechanical strength improved after the addition of Zn nanoparticle-doped flux before and after electromigration as compared to the undoped SAC305 solder joint. The Cu migration was suppressed by Zn nanoparticle doped due to which the fractured path was not shifted from the solder bulk to the cathode side. In comparison, the undoped solder showed rapid Cu migration due to which the fracture path shifted from solder bulk to cathode interface.

Address correspondence to E-mail: mnasir@ceme.nust.edu.pk

https://doi.org/10.1007/s10854-022-09722-4

1 Introduction

According to the environmental protection agency (EPA), both lead itself and compounds containing lead are very dangerous for the human health [1, 2]. The lead was included in the top seventeen chemicals that pose the greatest threat to human life and society. On 1st July 2006, the European community waste electrical and electronic equipment (WEEE) banned lead-based solder joints and led to a focus on the development of lead-free solder joints [3]. Lead plays an important role in Sn–Pb solder. It reduces the surface energy, interfacial energy, and brittleness of the Sn–Pb solder joints. It minimizes the Sn whisker growth and Sn pest [4]. It improves the wettability and reduces the reaction rate between the solder and under bump metallization [4].

The replacement of lead-based solder joints should have at least equal or better material properties such as mechanical, electrical, thermal, and structural properties than Sn–Pb solder. Because of the good reaction ability with the many metals, formation of intermetallic compound and low-temperature soldering, researchers suggested that Sn-based solder is one of the good replacement options of the Sn–Pb solder joint [5–14]. The Sn-based solder alloys include Sn–Ag–Cu, Sn–Ag–Zn, Sn–Cu, Sn–Ag, Sn–Zn [15], Ag–Bi and Sn–Bi [16], Sn–Ag, Sn–Cu, Sn–Bi, Sn–In, Sn–Zn, Sn–Sb, and Sn–Ge. Out of these solder joints, Sn-3.0Ag-0.5Cu (SAC305) solder joint was found to be one of the good candidate due to its good mechanical and electrical properties [17]. In this study SAC305 solder has been used.

The downscaling of electronic devices reduced the size of interconnects and increased the input current density in the solder joint [18, 19], which caused electromigration (EM) failures in the solder joint [4, 20, 21]. The current wind collides and scatters with the Cu atom present at the interfaces of the solder joint. Due to this, the Cu atoms migrate rapidly from the cathode side to the anode side of the solder joint [22]. The cathode interfaces become weak due to the voids formation after Cu migration. This causes the fracture pattern to be transferred from the solder bulk to the cathode side [23, 24]. It also changes the fracture mode from ductile to brittleness which decreases the strength of solder joint [25, 26].

To reduce these EM damages, numerous efforts were made in the past. Past studies used different techniques to modify the solder, such as adding alloying elements [27, 28], microparticles [29–31], and nanoparticles (NPs) [32–35]. Recently, another solder modification technique was developed which uses the NP-doped flux and mainly focuses on interfaces of solder joints [36–38]. As the EM failure occurs at the solder interfaces, this NP-doped flux technique allows us to study the interfacial intermetallic compounds (IMC). In earlier investigations, this approach added metallic NPs to lead-free solders [39–42]. It was observed that during the reflow process, reactive dissolution of metallic NPs took place, which increased the solder joint's properties. Bashir et al. found that the EM failures were reduced when Ni and Co NPs were added to the SAC305 solder joint [23, 33, 43]. Chan et al. studied that Zn particles also impact the interfacial IMCs in solder joints during reflow [41]. In past studies, researcher found that the addition of Zn NPs improved the microstructure and mechanical properties of the solder joint [41, 44, 45]. But no study was done to investigate the effect of Zn NP on electromigration failures. Henceforth, further research is needed to determine the effects of adding Zn NP-doped flux to the SAC305 solder joint during the EM test. This study aimed to investigate the effects of Zn NP-doped flux in the SAC305 solder joints on mechanical properties after the reflow process and EM test.

2 Methodology

The NP-doped flux was made by mixing a water-soluble flux with 2-wt% Zn NPs. 2 wt% of Zn NPs was mechanically mixed for 30 min with the flux. The average size of Zn NP was 25 ± 5 nm. Two copper wires with a length of 12 mm and a diameter of 0.5 mm were used. The wires were cleaned and polished from one end. To remove any oxide from wires, 10% H_2SO_4 and distilled water were used. The sample was kept in the solution for 30 s. After that, the polished ends of both wires were carefully dipped into the flux so that flux remained at the end of the wires and placed on the aluminium die. A 0.5-mm solder disk of SAC305 with a thickness of 2 mm was inserted between the cleaned ends of the copper wires. The sample was then reflowed in the reflow oven at 245°C for 45 s and a line-type solder joint is prepared as shown in Fig. 1. Further details of the sample preparations are given in our previous studies [23, 36, 46].

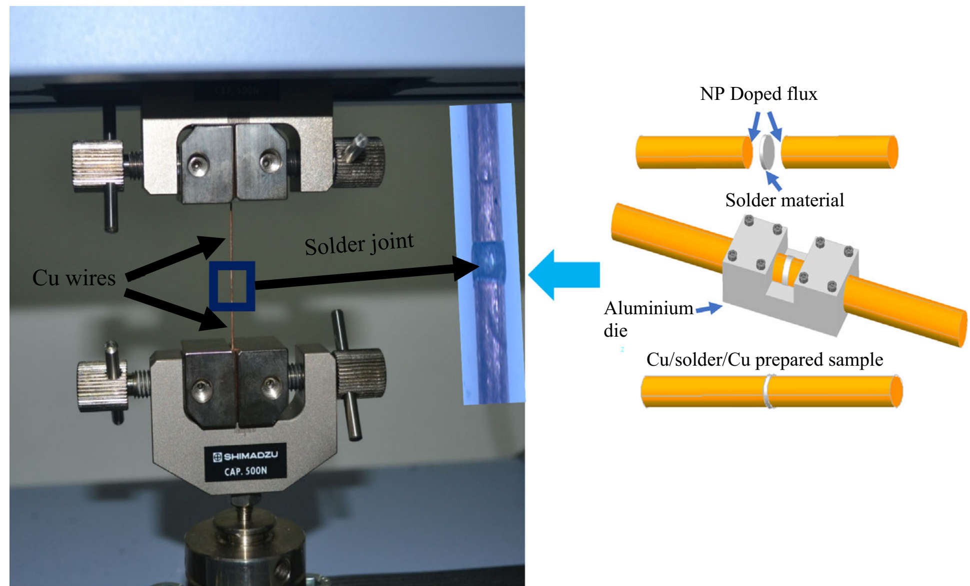

Fig. 1 Preparation of line-type Cu/solder/Cu sample

After reflow, the EM test was run. The samples were kept in a silicon oil bath to maintain the temperature at 80 ± 5 °C. For the EM test, a 5-A DC current was applied for a period of 192 h. After the EM test, tensile tests were carried out on a solder joint in a Shimadzu AGS-X Universal tensile testing machine using a 50-N load cell. The tests were repeated 5 times at a strain rate of $6.59 \times 10^{-5}\ s^{-1}$. During testing, stress–strain curves and ultimate tensile strength were obtained.

3 Results and discussion

Figure 2 shows the SEM images of interfaces for the SAC305 and SAC305 + 2-wt% Zn NP-doped solder joint. The common scallop-type Cu_6Sn_5 IMCs were found at both interfaces of the SAC305 sample [23]. After the addition of Zn NP-doped flux, the minor influence of Zn NP-doped was observed on the interfaces. The interfacial IMC thickness was slightly reduced [44]. Some $Cu_6(Sn, Zn)_5$ particles were also observed in the solder matrix and near the substrate.

Leong et al. discovered that adding Zn particles to SAC105 solder increased the amount of scallop-type Cu_6Sn_5 IMC after reflow [45]. Chan et al. observed that the interfacial IMC thickness of Cu_6Sn_5 was decreased after adding Zn NP to SAC387 using the paste mixing technique [41]. Park et al. discovered that by electroplating Zn NP on Cu pads in SAC305, the thickness of Cu_6Sn_5 was decreased after reflow [44]. Due to a small amount of Zn NP being dissolved during reflow in Cu_6Sn_5, they also discovered $Cu_6(Sn, Zn)_5$ IMC at the SAC/Cu–Zn interfaces.

Optical micrographs of SAC305 and SAC305 + 2-wt% Zn NP solder joints after EM tests are shown in Fig. 3. Samples 1 and 2 for the SAC305 solder joint exhibited the brittle fracture at the interfaces after 192 h of EM test. In our previous studies, it was detected that as reflowed SAC305 solder joint exhibited cup-and-cone fracture at the solder matrix. But in the current study, the EM process of Cu atoms weakened the cathode interface due to which the fracture path was found to be on the cathode interface, and the ductility changed to brittleness. In the case of the Zn NP-doped solder joint, the fracture remained in the solder matrix and did not shift to the cathode interface as shown in Fig. 3. Addition of Zn NP-doped maintained the ductility of the solder joint after the EM.

Bashir et al. studied the effects of Co and Ni addition in SAC305 solder joint after EM [36, 46]. They found that the SAC305 solder joint after the EM test exhibited a brittle fracture and the fracture path was shifted from the solder bulk to the cathode side after 192 h of the EM test. After the addition of Co NP, the fracture remained in the solder bulk after 192 h of the EM test. Similar results were also found by Ren et al. when reflowed samples of SAC387 solder joints were subjected to an EM test [25]. Other studies also found that the fracture path was shifted to the cathode side after the EM test in the Sn-3.8Ag-

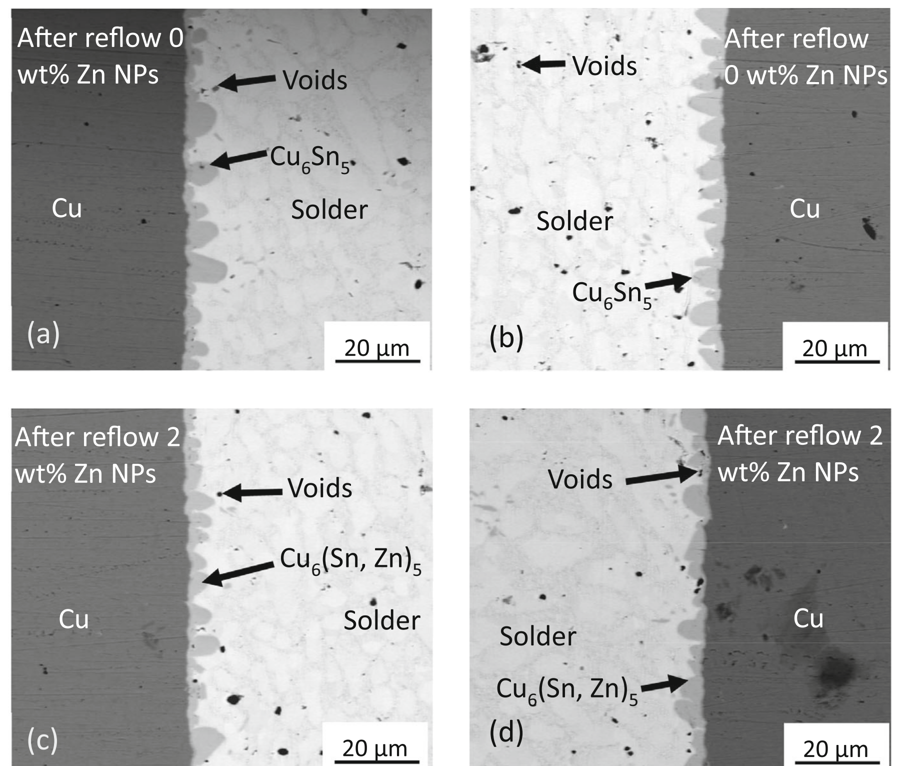

Fig. 2 **a**, **b** show SEM images of the cathode and anode side of the SAC305 sample, and **c**, **d** show the cathode and anode side of the SAC305 + 2-wt% Zn sample, respectively

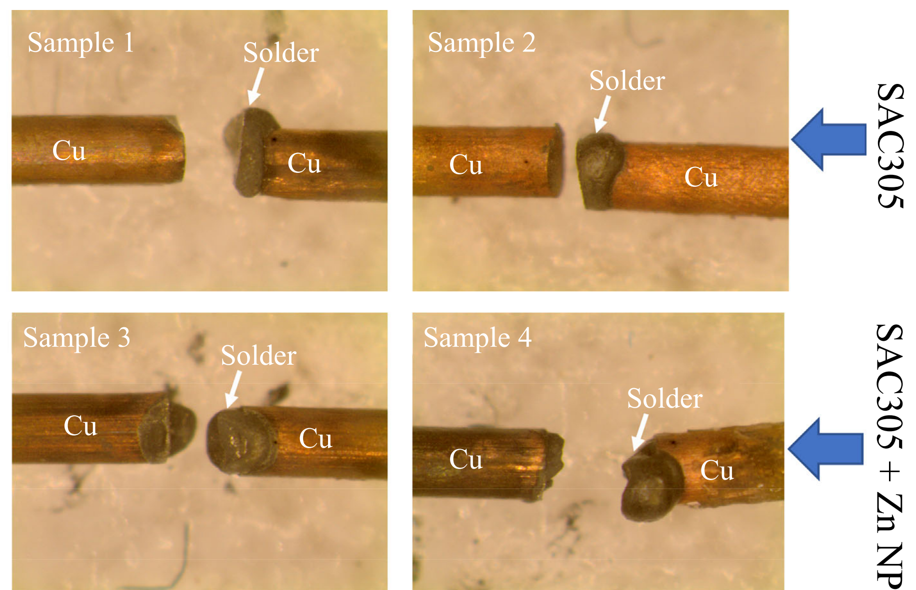

Fig. 3 Optical micrographs of tensile fracture for SAC305 and SAC305 + Zn NP

0.7Cu solder joint [47]. This is due to the formation of voids and cracks at the cathode side, which causes EM damage in the solder joint. The addition of Zn NP-doped flux has been found to suppress the EM damages at the cathode side.

Figure 4 shows the stress–strain curves at 0 and 192 h of the EM test of the SAC305 solder joint and SAC305 + 2-wt% Zn NP solder joint. Figure 4a shows the stress–strain curve of the SAC305 solder joint at 0 h of the EM test. The stress values range from 58 to 63 N/mm^2 at 0 h for all samples of the SAC305 solder joint. From the curves, the SAC305 solder joint exhibits plastic deformation. The strain values are higher than 0.6% for most of the samples.

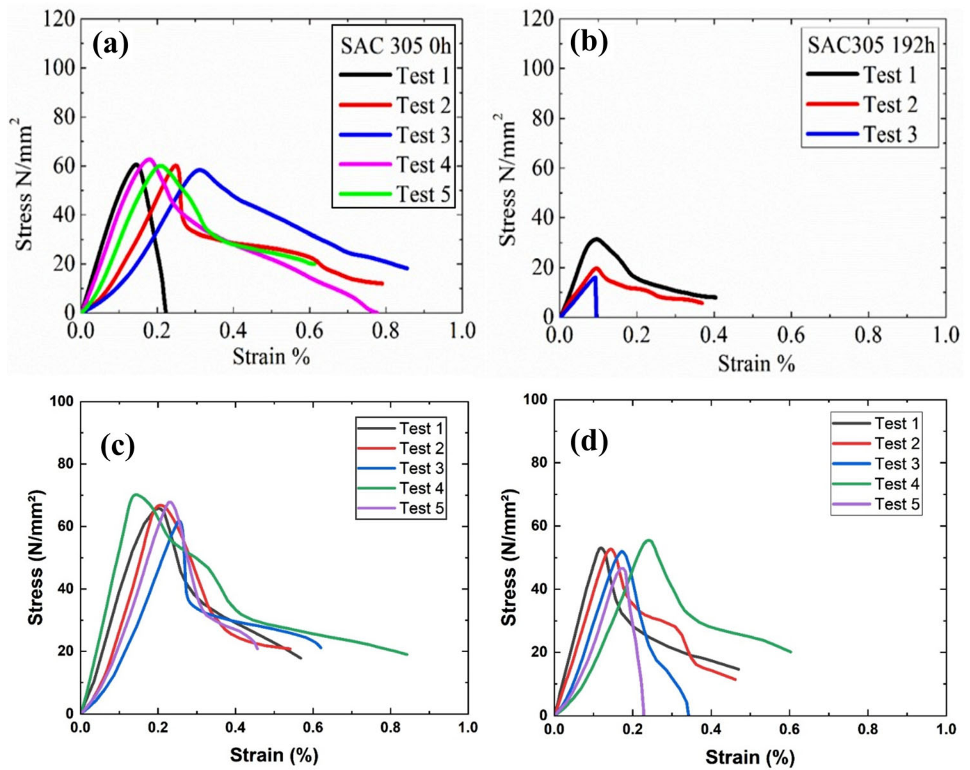

Fig. 4 Stress–strain curves of **a**, **b** SAC305 solder joint at 0 and 192-h EM [16], **c**, **d** SAC305 + 2-wt% Zn NP solder joint at 0- and 192-h EM test

Figure 4b shows the stress–strain curve of the SAC305 solder joint at 192 h of the EM test. The figure exhibits that all the samples of SAC305 solder joint were broken below the stress value of 35 N/mm^2. Figure 4c shows the stress–strain curve of SAC305 + 2-wt% Zn NP solder joint at 0 h of the EM test. The stress values range from 60 to 70 N/mm^2 at 0 h for all samples and strain values are less than 0.6% for most of the samples. From the curves, the SAC305 + 2-wt% Zn NP solder joint exhibited ductile fracture. Figure 4d shows the stress–strain curve of SAC305 + 2-wt% Zn NP solder joint at 192 h of the EM test. The stress of SAC305 + 2-wt% Zn NP solder joint was decreased after 192 h of the EM test. The stress values range from 45 to 55 N/mm^2 at 192 h for all samples of SAC305 + 2-wt% Zn NP solder joint. The stress values of SAC305 + 2-wt% Zn NP were higher than the SAC305 solder joint at 192 h of the EM test.

It was found that the stresses were higher after the addition of Zn NP doped to the SAC305 solder joint. Bashir et al. found that adding Ni NP to the SAC305 solder joint increases the stress compared to the SAC305 solder joint at 0 h of EM [46]. The stress was decreased after 192 h of EM for Ni NP-added solder but the reduction was lower than the SAC305 solder joint. Similar results were also found by Bashir et al. when Co NP was added to the SAC305 solder joint [36]. As a result, Zn NP-doped solders showed higher stresses after EM and the fracture behaviour was found to be ductile.

Figure 5 shows the ultimate tensile strength (UTS) at 0 and 192 h of the EM test for SAC305, SAC305 + 2-wt% Zn NP, SAC305 + 2-wt% Ni NP [46], and SAC305 + 2-wt% Co NP [36] solder joint.

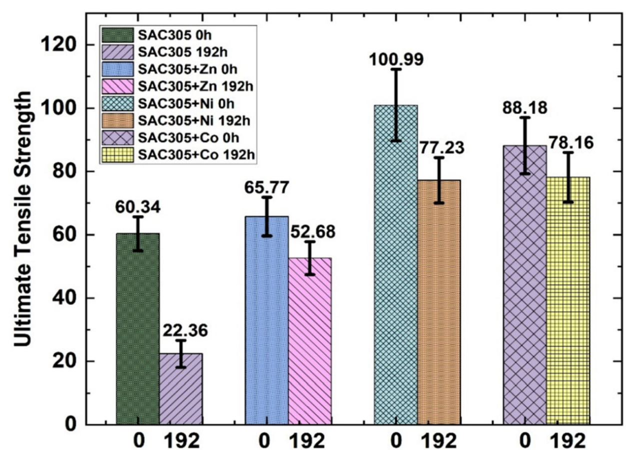

Fig. 5 Ultimate tensile strength of SAC305, SAC305 + 2-wt% Zn NP, SAC305 + 2-wt% Ni NP [24], and SAC305 + 2-wt% Co NP [16] solder joints at 0- and 192-h EM test

The average value of UTS for the SAC305 solder joint at 0 h was 60.34 N/mm^2 and after 192 h of EM was 22.36 N/mm^2. The UTS was drastically decreased after 192 h of EM for the SAC305 solder joint. The average value of UTS for SAC305 + 2-wt% Zn NP solder joint at 0 h was 65.7 N/mm^2 and after 192 h of EM was 52.68 N/mm^2. The UTS was not drastically decreased after 192 h of EM. The average values of UTS for SAC305 + 2-wt% Ni NP and SAC305 + 2-wt% Co NP solder joint at 0 h were 100.99 N/mm^2 and 88.18 N/mm^2, respectively. While, the average values of UTS for SAC305 + 2-wt% Ni NP and SAC305 + 2-wt% Co NP solder joint at 192 h of EM were 77.23 N/mm^2 and 78.16 N/mm^2, respectively. This showed that the Zn NP, Ni NP, and Co NP containing solder joints had higher UTS as compared to the UTS of the SAC305 solder joint at 0 and 192 h of EM test. The UTS of the SAC305 solder joint was decreased by 63%, while UTS of Zn NP, Ni NP, and Co NP containing solder joints were decreased only by 20%, 24%, and 11%, respectively.

From Fig. 5, it has been found that UTS significantly reduced in the SAC305 solder joint after 192 h of EM. The UTS of SAC305 was less than the SAC305 + 2-wt% Zn NP solder joint at 0 h of EM, while the ductility of SAC305 + 2-wt% Zn NP solder joint was less than the SAC305 solder joint. The UTS of SAC305 + 2-wt% Zn NP solder joint was reduced after 192 h of EM. The reduction of UTS in the SAC305 + 2-wt% Zn NP solder joint after 192 h of EM was also less than the SAC305 solder joint. After the addition of Zn NP, degradation in the UTS was suppressed after the EM test. Bashir et al. found that when Ni NP was added to the SAC305 solder joint, the tensile strength was increased at 0 h of EM as compared to the SAC305 solder joint [46] as shown in Fig. 5. The tensile strength after 192 h of EM was reduced, but the reduction was less than the SAC305 solder joint. Bashir et al. also found that after the addition of Co NP to the SAC305 solder joint, the tensile strength was increased at 0 h of EM but decreased after 192 h of EM and the reduction was lower than the SAC305 solder joint [36] as shown in Fig. 5. As a result, the solder joints with Zn NP added have a significant persistence of UTS.

4 Conclusion

The effects of Zn NP-doped flux on the mechanical properties of the SAC305 solder joint under high current were examined. SAC305 and SAC305 + 2-wt% Zn samples were prepared and an EM test was conducted. The results showed that before the EM test, the mechanical strength was improved after the addition of Zn NP-doped flux. After the EM test, the reduction in mechanical strength was controlled for the Zn NP-doped flux samples. The fractured path did not shift from the solder bulk to the cathode side after EM in SAC305 + 2-wt% Zn NP-doped solder joint. In SAC305 + 2-wt% Zn NP-doped solder joint, the fracture was found to be ductile at 0 h and remained ductile after the EM test for 192 h.

Acknowledgements

The authors gratefully thank and acknowledge the financial support from the University of Malaya and the Ministry of Higher Education, Malaysia.

Author contributions

All authors equally contributed to the conception and design, material selection, sample preparation, experiments, characterization, data collection, data analysis, and manuscript preparation.

Data availability

The current study is based on experimental data. In the manuscript, the experimental data were correlated and discussed with existing studies done by other researchers (given in the references). The experimental data of the current study are unpublished and will be provided when required.

Declarations

Competing interest The authors have no relevant financial interests to disclose.

Ethical approval The authors followed the ethical standards during the experiments as well as during the preparation of the manuscript.

References

1. J.F. Ziegler, Terrestrial cosmic rays. IBM J. Res. Dev **40**(1), 19–39 (1996)
2. K. Tu, A. Gusak, M. Li, Physics and materials challenges for lead-free solders. J. Appl. Phys **93**(3), 1335–1353 (2003)
3. S. Kumar, J. Jung, Mechanical and electronic properties of Ag 3 Sn intermetallic compound in lead free solders using ab initio atomistic calculation. Mater. Sci. Eng.: B **178**(1), 10–21 (2013)
4. Y.-D. Lu et al., Polarity effect of electromigration on intermetallic compound formation in SnPb solder joints. Acta Mater **57**(8), 2560–2566 (2009)
5. C. Wu et al., Properties of lead-free solder alloys with rare earth element additions. Mater. Sci. Eng.: R: Rep **44**(1), 1–44 (2004)
6. M. Abtew, G. Selvaduray, Lead-free solders in microelectronics. Mater. Sci. Eng.: R: Rep **27**(5), 95–141 (2000)
7. U.S. Mohanty, K.-L. Lin, Corrosion behavior of Pb-Free Sn-1Ag-0.5 Cu-XNi solder alloys in 3.5% NaCl solution. J. Electron. Mater **42**(4), 628–638 (2013)
8. J. Chen et al., Influence of minor Bi additions on the interfacial morphology between Sn–Zn–xBi solders and a Cu layer. J. Mater. Sci.: Mater. Electron **20**(11), 1112–1117 (2009)
9. L. Zhang et al., Development of Sn–Zn lead-free solders bearing alloying elements. J. Mater. Sci.: Mater. Electron **21**(1), 1–15 (2010)
10. J.H. Lau, *Flip chip technologies* (McGraw-Hill Professional, 1996)
11. K. Zeng, K.N. Tu, Six cases of reliability study of Pb-free solder joints in electronic packaging technology. Mater. Sci. Eng.: R: Rep **38**(2), 55–105 (2002)
12. S. Tonapi et al., Reliability of lead-free solder interconnects-a review, in *Reliability and maintainability symposium, 2002.* (IEEE, 2002)
13. V. Igoshev, J. Kleiman, Creep phenomena in lead-free solders. J. Electron. Mater **29**(2), 244–250 (2000)
14. J. Glazer, Microstructure and mechanical properties of Pb-free solder alloys for low-cost electronic assembly: a review. J. Electron. Mater **23**(8), 693–700 (1994)
15. H.R. Kotadia, P.D. Howes, S.H. Mannan, A review: on the development of low melting temperature Pb-free solders. Microelectron. Reliab **54**(6–7), 1253–1273 (2014)
16. N.C. Lee, *Getting ready for lead-free solders* (Soldering and Surface Mount Technology, 1997)
17. X. Zhang et al., Inhibition of electromigration in eutectic SnBi solder interconnect by plastic prestraining. J. Mater. Sci. Technol. **27**(11), 1072–1076 (2011)
18. M. Huang et al., Different diffusion behavior of Cu and Ni undergoing liquid–solid electromigration. J. Mater. Sci. Technol. **30**(12), 1235–1242 (2014)
19. D. Straubinger, T. Hurtony, A. Géczy, Impact of electromigration and isothermal ageing on lead-free solder joints of chip-sized SMD components. J. Mater. Res. Technol. **21**, 308–318 (2022)
20. J. Qiao et al., Characteristics of stress relaxation kinetics of La60Ni15Al25 bulk metallic glass. Acta Mater **98**, 43–50 (2015)
21. H. He et al., Bi layer formation at the anode interface in Cu/Sn-58Bi/Cu solder joints with high current density. J. Mater. Sci. Technol. **28**(1), 46–52 (2012)
22. P. Liu et al., Fast and huge anisotropic diffusion of Cu (Ag) and its resistance on the Sn self-diffusivity in solid β–Sn. J. Mater. Sci. Technol. **32**(2), 121–128 (2016)
23. M.N. Bashir et al., Reduction of electromigration damage in SAC305 solder joints by adding Ni nanoparticles through flux doping. J. Mater. Sci **50**(20), 6748–6756 (2015)
24. M. Li et al., Materials modification of the lead-free solders incorporated with micro/nano-sized particles: a review. Mater. Design **197**, 109224 (2021)
25. F. Ren et al., Electromigration induced ductile-to-brittle transition in lead-free solder joints. Appl. Phys. Lett **89**(14), 141914 (2006)
26. P. Zhang, S. Xue, J. Wang, New challenges of miniaturization of electronic devices: electromigration and thermomigration in lead-free solder joints. Mater. Design **192**, 108726 (2020)
27. Y. Wang, C. Chang, C. Kao, Minimum effective ni addition to SnAgCu solders for retarding Cu3Sn growth. J. Alloys Compd **478**(1–2), L1–L4 (2009)
28. C. Wang, S. Huang, K. Li, Inhibiting CoSn3 growth at the Sn/Co system by minor Zn addition. Intermetallics **56**, 68–74 (2015)
29. R. Zhang et al., Electromigration in Sn-Bi modified with polyhedral oligomeric silsesquioxane. J. Electron. Mater **39**(12), 2513–2521 (2010)
30. H. Rhee et al., Effects of intermetallic morphology at the metallic particle/solder interface on mechanical properties of Sn-Ag-based solder joints. J. Electron. Mater **32**(11), 1257–1264 (2003)
31. M.N. Bashir et al., Effects of tin particles addition on structural and mechanical properties of eutectic Sn–58Bi solder joint. J. Mater. Sci.: Mater. Electron. **2022**, 1–9 (2022)
32. F. Guo, G. Xu, H. He, Electromigration behaviors in Sb particle-reinforced composite eutectic SnAgCu solder joints. J. Mater. Sci **44**(20), 5595–5601 (2009)
33. M.N. Bashir, A. Haseeb, Grain size stability of interfacial intermetallic compound in Ni and Co nanoparticle-doped

SAC305 solder joints under electromigration. J. Mater. Sci.: Mater. Electron. **2022**, 1–9 (2022)
34. J. Wu et al., Recent progress of Sn–Ag–Cu lead-free solders bearing alloy elements and nanoparticles in electronic packaging. J. Mater. Sci.: Mater. Electron **27**(12), 12729–12763 (2016)
35. M. Nasir Bashir et al., Effect of cobalt nanoparticles on mechanical properties of Sn–58Bi solder joint. J. Mater. Sci.: Mater. Electron. **2022**, 1–7 (2022)
36. M.N. Bashir et al., Effect of cobalt doping on the microstructure and tensile properties of lead free solder joint subjected to electromigration. J. Mater. Sci. Technol. **32**(11), 1129–1136 (2016)
37. G. Sujan, A. Haseeb, A. Afifi, Effects of metallic nanoparticle doped flux on the interfacial intermetallic compounds between lead-free solder ball and copper substrate. Mater. Charact **97**, 199–209 (2014)
38. A. Aspalter et al., Hybrid solder joints: morphology and shear strength of Sn–3.0 Ag–0.5 Cu solder joints by adding ceramic nanoparticles through flux doping. Appl. Nanosci. **10**(12), 4943–4949 (2020)
39. S. Tay et al., Influence of Ni nanoparticle on the morphology and growth of interfacial intermetallic compounds between Sn–3.8 Ag–0.7 Cu lead-free solder and copper substrate. Intermetallics **33**, 8–15 (2013)
40. A. Haseeb, T.S. Leng, Effects of Co nanoparticle addition to Sn–3.8 Ag–0.7 Cu solder on interfacial structure after reflow and ageing. Intermetallics **19**(5), 707–712 (2011)
41. Y. Chan, M. Arafat, A. Haseeb, *Effects of reflow on the interfacial characteristics between Zn nanoparticles containing Sn-3.8 Ag-0.7 Cu solder and copper substrate* (Soldering and Surface Mount Technology, 2013)
42. A. Haseeb, M. Arafat, M.R. Johan, Stability of molybdenum nanoparticles in Sn–3.8 Ag–0.7 Cu solder during multiple reflow and their influence on interfacial intermetallic compounds. Mater. Charact **64**, 27–35 (2012)
43. M.N. Bashir et al., Effect of Ni and Co nanoparticle-doped flux on microstructure of SAC305 solder matrix. J. Mater. Sci.: Mater. Electron. **2022**, 1–15 (2022)
44. J.Y. Park et al., Electromigration reliability of Sn–3.0 Ag–0.5 Cu/Cu–Zn solder joints. J. Mater. Sci.: Mater. Electron **30**(8), 7645–7653 (2019)
45. Y. Leong et al., Microstructure and mechanical properties of Sn–1.0 Ag–0.5 Cu solder with minor zn additions. J. Mater. Sci.: Mater. Electron **30**(13), 11914–11922 (2019)
46. M.N. Bashir, A. Haseeb, Improving mechanical and electrical properties of Cu/SAC305/Cu solder joints under electromigration by using Ni nanoparticles doped flux. J. Mater. Sci.: Mater. Electron **29**(4), 3182–3188 (2018)
47. X. Wang et al., Effects of current stressing on shear properties of Sn-3.8 Ag-0.7 Cu solder joints. J. Mater. Sci. Technol. **26**(8), 737–742 (2010)

Publisher's Note Springer Nature remains neutral with regard to jurisdictional claims in published maps and institutional affiliations.

Springer Nature or its licensor (e.g. a society or other partner) holds exclusive rights to this article under a publishing agreement with the author(s) or other rightsholder(s); author self-archiving of the accepted manuscript version of this article is solely governed by the terms of such publishing agreement and applicable law.